

Local Rendezvous Hashing: Bounded Loads and Minimal Churn via Cache-Local Candidates

Yongjie Guan
Zhejiang University of Technology

December 30, 2025

Abstract

Consistent hashing is fundamental to distributed systems. Classical ring-based schemes offer stability under updates but can exhibit a peak-to-average load ratio (PALR) of $\Theta(\ln n)$ in the single-token regime; achieving PALR of $1+\varepsilon$ requires $\Theta(\ln n/\varepsilon^2)$ virtual nodes per physical node in widely-used analyses [4]. Multi-probe consistent hashing (MPCH) achieves near-perfect balance with $O(1/\varepsilon)$ probes [4], but its probes typically translate into scattered memory accesses.

We introduce **Local Rendezvous Hashing (LRH)**, which restricts Highest Random Weight (HRW) selection [18, 19] to a contiguous window of C *distinct* physical neighbors on a ring. Precomputed *next-distinct* offsets make candidate enumeration *exactly C ring steps* (distinct nodes), while the overall lookup remains $O(\log |\mathcal{R}| + C)$ due to the initial binary search. In a large-scale benchmark with $N=5000$ nodes, $V=256$ vnodes/node, $K=50M$ keys, $C=8$ (20 threads), LRH reduces PALR (Max/Avg) from 1.2785 to 1.0947 and empirically enforces $\text{ScanMax} = C$ under fixed-candidate enumeration. Under fixed-candidate liveness failover, LRH achieves 0% excess churn. Compared to MPCH(8 probes), LRH achieves $\approx 6.8 \times$ higher throughput (60.05 vs 8.80 M keys/s) while approaching MPCH’s load balance. A microbenchmark further shows that speeding up MPCH probe generation by $4.41 \times$ improves assign-only throughput by only $1.06 \times$, confirming that MPCH remains dominated by $P \times$ lower-bound ring memory traffic rather than hash arithmetic.

1 Introduction

Partitioning keys uniformly across a changing set of nodes underpins sharded caches, distributed storage, and load balancers (e.g., Dynamo [6], Maglev [8]). An ideal assignment function must jointly satisfy:

1. **Uniformity:** load should be balanced (PALR, P99/Avg).
2. **Minimal churn:** only necessary keys move on changes.
3. **Performance:** lookups must be fast and cache-friendly.

In practice these objectives conflict. Ring consistent hashing [9] is stable, but can be imbalanced without enough vnodes [4]. MPCH improves balance using multiple probes [4], but implies additional probe lookups and memory touches. Maglev [8] uses a lookup table for near-perfect balance yet explicitly tolerates a small number of table disruptions under backend changes. Recent consistent hashing systems such as ANCHORHASH aim for high performance and strong consistency properties under arbitrary membership changes [13].

Our goal. We focus on a common setting in high-throughput data planes: *fast per-key lookup with bounded work, cache locality, and minimal churn under liveness failures*. We propose LRH: keep the ring topology but *smooth local imbalance* by running a small HRW election among C cache-local distinct candidates.

Contributions.

- **LRH algorithm:** HRW election within a ring-local window of C distinct nodes.
- **Next-distinct offsets:** enforce bounded distinct candidate enumeration in exactly C ring steps.
- **Liveness failures with minimal churn:** fixed-candidate filtering yields 0% excess churn under topology-fixed failures.
- **Weighted extension:** topology-weight decoupling via weighted HRW as standardized in an IETF draft [3].
- **Large-scale evaluation:** $N=5000$, $V=256$, $K=50M$, multiple failure sizes and repeats, with detailed churn and concentration metrics.

2 Background and Problem Setting

2.1 Two kinds of “changes”: membership vs liveness

We distinguish two operational regimes:

Membership change. Nodes are added/removed from the configuration. Data structures may change

(ring rebuild, table rebuild, etc.). This may induce churn beyond the theoretical minimum, depending on algorithm design [8, 13].

Live ness change. Nodes temporarily fail/recover, while the configured topology remains fixed (e.g., alive mask changes). Many systems strongly prefer minimal movement under such failures because failures may be frequent and transient.

Our strongest churn guarantee is for *liveness changes* with fixed topology (Theorem 1).

2.2 Ring hashing, vnodes, and imbalance

Ring consistent hashing maps nodes (or vnodes) to tokens on the unit circle and assigns keys to the next token clockwise [9]. Analyses in MPCH show that in the one-token setting the maximum gap is $\Theta(\ln n/n)$, yielding PALR $\Theta(\ln n)$; and to achieve $\text{PALR} \leq 1+\epsilon$ requires $\Theta(\ln n/\epsilon^2)$ vnodes per node [4]. Large vnode state can stress memory and caches in high-throughput implementations. Our vnode sweep (Section 6.8) empirically quantifies this trade-off: higher V improves balance but substantially increases ring build cost and reduces lookup throughput.

2.3 HRW (Rendezvous hashing)

HRW [19] assigns each key to the node maximizing a hash-derived score. It achieves strong balance but costs $O(N)$ work per key if performed over all nodes.

2.4 MPCH and Maglev

MPCH [4] reduces imbalance using K probes per key. In a typical implementation, each probe implies additional index lookups; performance can suffer when the probes translate into scattered memory accesses (a practical point also highlighted when contrasting ring/vnode tables vs other approaches) [12].

Maglev [8] builds a lookup table of size M for fast dispatch, achieving near-perfect balance; it tolerates a small disruption rate under backend changes and discusses the trade-off between table size, disruption, and build cost.

2.5 Where LRH fits among modern alternatives

Two influential directions:

CH-BL (bounded loads). CH-BL augments CH with capacity constraints and forwarding to bound maximum load while controlling expected moves under updates [14].

AnchorHash. ANCHORHASH achieves strong consistency and high performance under arbitrary membership changes without large vnode state [13]. LRH, in

contrast, is *ring-preserving*: it keeps an existing token ring and adds only a per-entry next-distinct offset plus a C -way HRW election over ring-local distinct candidates. This targets deployments where failures are treated as liveness changes (fixed topology) and ring compatibility/cache-local bounded work are primary constraints.

LRH is complementary: it keeps the ring topology (ease of integration) but introduces *cache-local elections* to improve balance with fixed bounded work.

3 Local Rendezvous Hashing (LRH)

3.1 Data Structure

Let $\mathcal{N} = \{0, \dots, N-1\}$ be physical node ids. The ring \mathcal{R} is a sorted array of $|\mathcal{R}| = N \cdot V$ entries:

$$\mathcal{R}[i] = (token_i, node_i, \delta_i),$$

sorted by $token_i$. The **next-distinct offset** δ_i satisfies:

$$\mathcal{R}[(i+\delta_i) \bmod |\mathcal{R}|].node \neq \mathcal{R}[i].node,$$

and is the smallest such positive offset (wrapping around).

3.2 Lookup

Given key k and candidate count C :

1. Compute $h = \text{HASHPOS}(k)$ and locate $idx = \text{LOWERBOUND}(\mathcal{R}, h)$.
2. Enumerate C distinct candidates by walking δ offsets.
3. Select the candidate with the maximum HRW score (or weighted score).

Bounded distinct enumeration. The next-distinct offsets guarantee *exactly C ring steps* to enumerate C distinct physical nodes, independent of vnode clustering. The remaining cost is the initial lower-bound search; hence total complexity is $O(\log |\mathcal{R}| + C)$.

Figure 1 shows that, under fixed-candidate enumeration, LRH empirically enforces ScanMax= C across failure sizes.

3.3 Building next-distinct offsets

Offsets are computed once per ring build (or rebuild). Let $R[i].node$ denote the node id.

This is $O(|\mathcal{R}|)$ time and $O(1)$ extra memory.

3.4 Weighted nodes (topology-weight decoupling)

To support heterogeneous capacities without rebuilding the ring, we use weighted HRW as standardized in an

Algorithm 1 LRH Lookup

```
1: function LOOKUP( $k, C$ )
2:    $h \leftarrow \text{HASHPOS}(k)$ 
3:    $idx \leftarrow \text{LOWERBOUND}(\mathcal{R}, h)$ 
4:    $best \leftarrow \text{null}; best\_s \leftarrow -\infty$ 
5:   for  $t \leftarrow 1$  to  $C$  do
6:      $e \leftarrow \mathcal{R}[idx]$ 
7:      $s \leftarrow \text{HASHSCORE}(k, e.\text{node})$ 
8:     if  $s > best\_s$  then
9:        $best\_s \leftarrow s; best \leftarrow e.\text{node}$ 
10:    end if
11:     $idx \leftarrow (idx + e.\delta) \bmod |\mathcal{R}|$ 
12:   end for
13:   return  $best$ 
14: end function
```

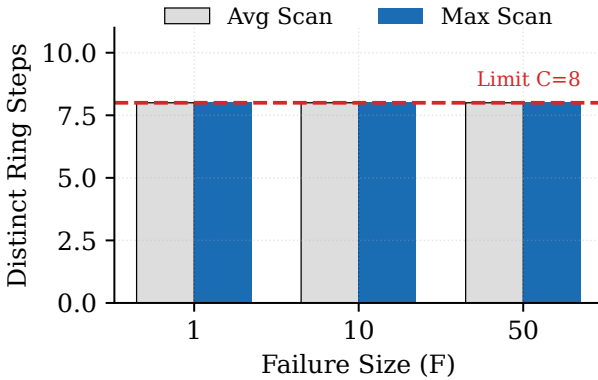


Figure 1: Bounded distinct enumeration evidence: under fixed-candidate enumeration, LRH empirically enforces ScanMax= C (here $C=8$) across failure sizes.

IETF draft [3] and commonly derived via exponential-race style constructions [7, 17]. One equivalent form is:

$$\arg \min_n \frac{-\ln(u_{k,n})}{w_n}, \quad u_{k,n} \sim \text{Unif}(0, 1).$$

Weights w_n reside in a separate array; updating weights is $O(1)$ and does not modify tokens.

3.5 Failure handling: fixed-candidate filtering

We define two modes:

Fixed-candidate (liveness failures). Compute the static candidate set S_k (size C) from the fixed ring; among S_k choose the highest-scoring *alive* node. This confines failover within a predetermined set.

All candidates down (rare) fallback. If all C candidates are down, extend the window by another block of C candidates (repeat) until finding an alive node or hitting an implementation cap (e.g., max-scan). This preserves availability; it may increase work only in extreme failure scenarios.

Algorithm 2 BuildNextDistinctOffsets

```
1: function BUILDNEXTDISTINCTOFFSETS( $R$ )
2:    $m \leftarrow |\mathcal{R}|$ 
3:    $j \leftarrow 1$ 
4:   for  $i \leftarrow 0$  to  $m-1$  do
5:     if  $j \leq i$  then
6:        $j \leftarrow i+1$ 
7:     end if
8:     while  $R[j \bmod m].\text{node} = R[i].\text{node}$  do
9:        $j \leftarrow j+1$ 
10:    end while
11:     $R[i].\delta \leftarrow (j-i)$ 
12:   end for
13: end function
```

4 Analysis

4.1 Complexity and memory

Time. Lookup is $O(\log |\mathcal{R}| + C)$: one lower-bound search on $|\mathcal{R}| = NV$ plus C next-distinct steps.

Space. Ring storage is $O(NV)$ entries. With $N=5000, V=256, |\mathcal{R}|=1.28M$.

4.2 Churn guarantee under liveness failures

Theorem 1 (Zero Excess Churn Under Fixed-Candidate Liveness Failures). *Assume the ring topology is unchanged and only node liveness changes. Under LRH fixed-candidate filtering, only keys whose original winner is now dead are remapped; therefore excess churn is zero.*

Proof sketch. For any key k , the candidate set S_k and the per-candidate scores are deterministic functions of (k, \mathcal{R}) . If the original winner remains alive, it still has the maximal score among alive candidates in S_k , so the mapping does not change. Only keys whose original winner is dead fail over to the best alive candidate in the same S_k . Thus no healthy keys move, implying zero excess churn. \square

4.3 Smoothing Effect Analysis of C -th Local Selection

What we claim vs. what we do not claim. LRH can be viewed as a *local multi-choice* mechanism: each key compares C *distinct* ring-local candidates and selects the maximum HRW score among them. Classical “power of two choices” results assume (nearly) i.i.d. global samples; LRH candidates are ring-local and hence correlated. Therefore:

- We **do not claim** a universal, assumption-free worst-case bound for all adversarial token layouts.
- We **do claim** a precise *smoothing identity* under score symmetry, and a clean *scaling law* under a standard randomized-ring regime.

In Appendix D, we explicitly bound the secondary effects omitted by the simplified model, including the ran-

domness of the candidate count d_n , discrete key sampling, and locality correlations.

Fluid model and notation. Let the ring contain $m = |\mathcal{R}| = NV$ tokens on $[0, 1)$. Let G_1, \dots, G_m be consecutive cyclic gap lengths with $\sum_{i=1}^m G_i = 1$. All keys hashing into the same gap share the same successor index and therefore the same LRH candidate set; denote by $S_i \subseteq \mathcal{N}$ the C distinct candidates associated with gap i .

Score symmetry. For a fixed key k , assume the per-node HRW scores $\{s(k, n)\}_{n \in S_i}$ are i.i.d. with a continuous distribution (e.g., produced by a keyed hash). Ties occur with probability 0.

Lemma 1 (Uniform winner within a fixed candidate set). *Fix a key k and a candidate set S with $|S| = C$. If $\{s(k, n)\}_{n \in S}$ are i.i.d. continuous, then for every $n \in S$,*

$$\Pr[\arg \max_{x \in S} s(k, x) = n] = \frac{1}{C}.$$

Proof. By exchangeability under relabeling, each of the C candidates is equally likely to be the unique maximizer. \square

A smoothing identity (structural). Let L_n be node n 's *fluid* load share (fraction of the unit circle mapped to n). Lemma 1 implies each gap contributes its mass evenly to all C candidates in its set:

$$L_n = \frac{1}{C} \sum_{i: n \in S_i} G_i. \quad (1)$$

Thus, relative to ring CH (where each gap maps entirely to one successor), LRH replaces “winner-takes-all” by a *local averaging operator* over C candidates.

Scaling law. Under a randomized-ring regime (i.i.d. uniform token positions), (1) yields the familiar variance scale $\text{SD}(L_n) \approx 1/(N\sqrt{VC})$ and the max-deviation scale $\text{PALR} = 1 + O(\sqrt{\ln N/(VC)})$. This confirms the \sqrt{C} smoothing gain observed in our evaluations.

Note on baseline fairness: V vs. VC (cost matters). The randomized-ring scaling suggests that LRH’s structural smoothing $\text{SD}(L_n) \propto 1/\sqrt{VC}$ matches ring CH if one simply increases vnodes to $V' = VC$. While statistically equivalent, the distinction is cost structure: ring CH pays $C \times$ state blow-up (ring size $NV \rightarrow NVC$), worsening cache/TLB locality and build overhead, whereas LRH keeps the ring size fixed at NV and pays an extra $O(C)$ *ring-local* work per lookup. Our vnode sweep (Section 6.8) empirically illustrates this trade-off.

4.4 Availability Analysis of p^C

What we claim vs. what we do not claim. Fixed-candidate liveness handling yields zero excess churn

(Theorem 1) but implies that availability depends on the joint failure probability of the candidate set. We presents models for independent failures and fixed-fraction failures. We **do not claim** intrinsic immunity to topology-correlated failures (e.g., rack failure) if tokens are placed naively; however, Appendix D.7 shows that with standard random hashing (which decorrelates logical position from physical ID), the probability of hitting a single point of failure decays exponentially in C .

Theorem 2 (Independent liveness model). *Assume each node is independently down with probability p . For any key k whose LRH candidate set S_k contains C distinct nodes, let A_k be the event that all C candidates in S_k are down. Then*

$$\Pr[A_k] = p^C, \quad \Pr[\overline{A_k}] = 1 - p^C.$$

Proof. Distinctness gives C independent down events; multiply probabilities. \square

Theorem 3 (Fixed- F failure model (hypergeometric)). *Suppose exactly F out of N nodes are down, and S_k behaves as a uniformly random C -subset of nodes. Then*

$$\Pr[S_k \subseteq \text{Failed}] = \frac{\binom{F}{C}}{\binom{N}{C}} \leq \left(\frac{F}{N}\right)^C.$$

Proof. Counting argument for the exact ratio; the inequality follows from

$$\frac{\binom{F}{C}}{\binom{N}{C}} = \prod_{j=0}^{C-1} \frac{F-j}{N-j} \leq (F/N)^C$$

. \square

Fallback cost. If the implementation extends the window by additional C -blocks until success, under independent failures the number of blocks is geometric:

$$\begin{aligned} \mathbb{E}[\#\text{blocks}] &= \frac{1}{1 - p^C}, \\ \mathbb{E}[\#\text{candidates examined}] &= \frac{C}{1 - p^C}. \end{aligned}$$

5 Implementation Notes

Hashing. Two hashes are used: HASHPOS determines ring position and HASHSCORE determines HRW score. In adversarial environments, these should be keyed (e.g., SipHash) [5] to prevent crafted keys from skewing balance.

Modes in evaluation. We evaluate several update/-failure semantics:

- **rebuild**: rebuild the structure after failures/membership change.
- **next-alive** (ring/mpch variants): keep topology and scan to the next alive node during lookup.
- **fixed-candidate** (LRH): compute a fixed candidate set and select the best alive within it.

These semantics matter: algorithms that rebuild can induce additional remapping (excess churn), while fixed-topology strategies can achieve zero excess churn for liveness changes (Theorem 1).

6 Evaluation

6.1 Experimental setup

Hardware/OS. Windows 11, Intel Ultra 7 265KF, 64 GB DDR5-6400.

Core parameters. $N=5000$ nodes, $V=256$ vnodes/node ($|\mathcal{R}|=1.28M$), $K=50,000,000$ keys, LRH candidates $C=8$, Maglev table size $M=65537$ (prime), failure sizes $\{1, 10, 50\}$, 5 repeats per failure size, 1 warmup.

Parallelism. All experiments use Rayon with 20 worker threads (reported by the benchmark) [16]. We report aggregate throughput across threads.

Workload generation. Keys are generated via a seeded PRNG (base seed 20251226; repeats use different derived seeds). The large K reduces sampling noise for distribution metrics.

Fairness and comparability. All schemes are evaluated under a shared harness: identical key generation, identical failure sets, and a unified metric implementation for moved/excess/affected/recv. We make evaluation semantics explicit in the results ([`rebuild`], [`next-alive`], [`fixed-cand`]), since failure-handling policy is part of the systems contract and directly affects churn. We also remove non-algorithmic overheads from timed regions where possible (e.g., allocating an `alive_all` vector outside the timed query loop) to avoid “implementation constant” bias.

Implementation scope and threats to validity. Our implementations are reference-level and prioritize semantic fidelity over peak optimization (e.g., limited use of prefetching, vectorization, or layout-specific tuning). Consequently, throughput results should be interpreted as prototype-level evidence and may vary under optimized production implementations, although the observed gaps are consistent with the algorithms’ differing memory-access patterns (sequential ring steps vs. scattered probes). Additionally, HRW uses key sampling for large N due to its $O(N)$ per-key cost, so its throughput is reported separately and is not directly comparable to full-key runs.

6.2 Baselines

We compare: Ring [9], MPCH [4], Maglev [8], Jump [12], HRW [19], and CRUSH [20]. Finally, we implement a *CRUSH-like* two-level rack model to serve as a structural baseline.

Note on Jump semantics. Jump Hash requires contiguous bucket IDs [12]. Our benchmark models a rebuild-by-renumber semantics under membership changes, which is not Jump’s intended sweet spot; we report results for transparency and to illustrate semantic sensitivity.

6.3 Metrics (exact definitions)

Let K_{used} be the number of keys actually evaluated in a row (e.g., sampled for full HRW).

- **Churn%** = $\frac{\text{moved}}{K_{\text{used}}} \times 100\%$, where moved counts keys with `init_idx` \neq `fail_idx`.
- **Excess%**: churn beyond the theoretical minimum for the given failure size (as computed by the benchmark harness).
- **FailAffected**: number of keys whose *initial* assignment fell into the failed node set (keys that truly require failover), not equal to moved.
- **MaxRecvShare** = $\max_i \frac{\text{recv}[i]}{\text{affected}}$, where `recv[i]` counts only *affected keys* remapped to alive node i .
- **Conc(\times)** = $\frac{\text{MaxRecvShare}}{1/N_{\text{alive}}}$, i.e., the busiest receiver’s share relative to ideal equal split among alive nodes.
- **ScanAvg**: average scan steps (each step checks the next token/candidate until hitting an alive node), computed as `scan_sum/denom`.
- **ScanMax**: maximum observed scan steps in any single mapping (init or fail).

6.4 Overall results (all failure sizes)

Table 1 reports the overall average across failure sizes (15 runs total). Figure 2 visualizes the throughput/balance trade-off across the evaluated methods.

Uniformity. Ring($vn=256$) has $\text{Max}/\text{Avg}=1.2785$. LRH reduces this to 1.0947 using only $C = 8$ distinct candidates, while MPCH ($P=8$) reaches 1.0697. Thus LRH approaches MPCH’s balance while keeping candidate enumeration local and strictly bounded.

Throughput and cache locality. LRH achieves 60.05 M keys/s, only about 13% below Ring(`next-alive`) at 68.95 M keys/s, indicating that the additional C candidate checks are largely cache-local. In contrast, MPCH shows a steep probe-driven trade-off: at $vn=256$, increasing probes from $P=2$ to $P=32$ improves imbalance from 1.1393 to 1.0471 but reduces throughput from 32.74 to 1.91 M keys/s. At comparable imbalance to LRH (e.g., MPCH $P=4$ at 1.0991), MPCH is still markedly slower (16.90 vs. 60.05 M keys/s), consistent with probe-driven scattered ring accesses.

MPCH sensitivity to ring size. Appendix Figure 10 fixes $P=8$ and varies $vn \in \{1, 16, 256\}$: MPCH operates without virtual nodes, but larger rings improve balance at a substantial throughput cost, consistent with ring footprint effects in addition to the dominant multi-probe lookup cost.

Table 1: Overall Average Across Failure Sizes (N=5000, V=256, K=50M; 15 runs total). HRW is reported on sampled keys; modes [rebuild]/[next-alive]/[fixed-cand] indicate different failure-handling semantics. Throughput is aggregate across 20 Rayon threads.

Algorithm	K used	Build (ms)	Query (ms)	Thrpt (M/s)	Max/Avg	P99/Avg	CV	Churn (%)	Excess (%)	FailAff	MaxRecv share	Conc (x)	ScanAvg/Max
Ring(vn=256)[rebuild]	50M	60.98	1303.94	38.36	1.2785	1.1550	0.0639	0.408	0.000	204044	0.0099	49.33	0.00/0
Ring(vn=256)[next-alive]	50M	0.00	725.34	68.95	1.2785	1.1550	0.0639	0.408	0.000	204044	0.0099	49.33	1.00/3
MPCH(ring,vn=256,P=8)[next-alive]	50M	28.69	5680.67	8.80	1.0697	1.0439	0.0192	0.407	0.000	203587	0.0020	10.08	8.02/11
LRH(vn=256,C=8)[fixed-cand]	50M	30.58	832.98	60.05	1.0947	1.0574	0.0244	0.407	0.000	203416	0.0012	6.14	8.00/8
LRH(vn=256,C=8)[rebuild]	50M	62.68	1509.80	33.16	1.0947	1.0574	0.0244	0.719	0.312	203416	0.0012	5.89	8.00/8
Jump[rebuild-buckets]	50M	0.00	202.47	248.09	1.0361	1.0232	0.0100	66.214	65.808	203140	0.3740	1868.90	0.00/0
Maglev(M=65537)[rebuild]	50M	2.98	38.51	1301.76	1.1000	1.0818	0.0257	1.971	1.565	202824	0.0334	166.72	0.00/0
HRW(sample K=2M)	2M	0.01	1723.36	1.16	1.1810	1.1185	0.0501	0.405	0.000	8106	0.0026	12.93	0.00/0
CRUSH-like(rack=50,bp=8,lp=8,tries=16)	50M	0.00	604.37	82.79	1.0379	1.0233	0.0100	0.406	0.000	203143	0.0005	2.58	16.03/57

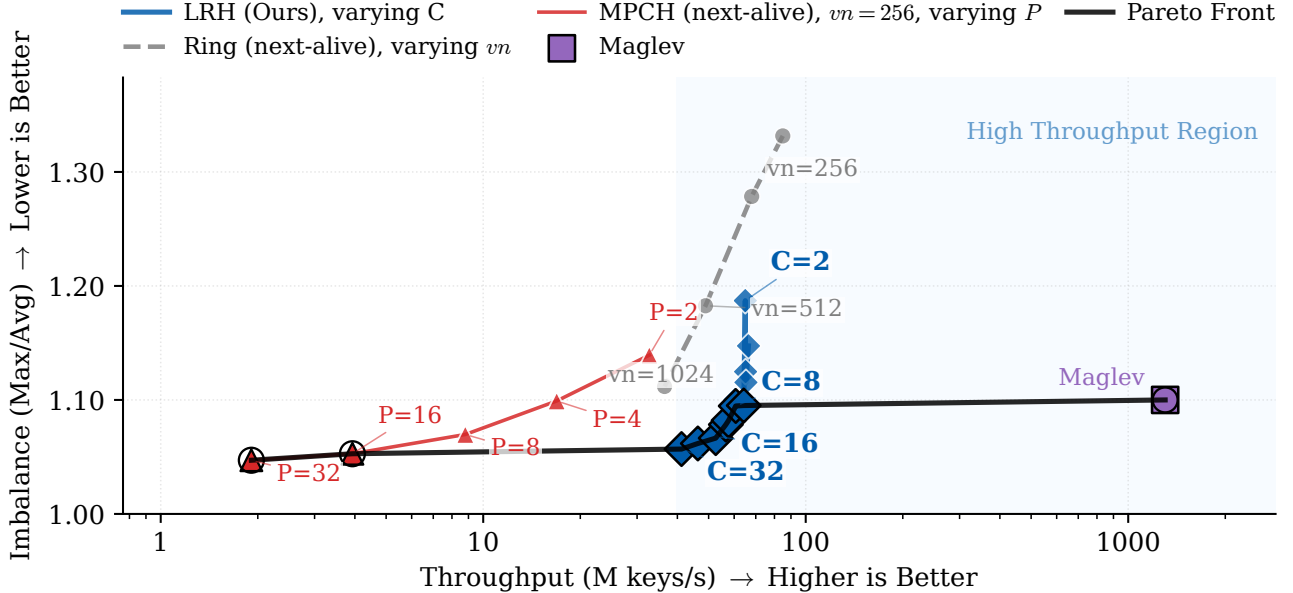


Figure 2: Throughput–imbalance trade-off (all failure sizes): throughput vs. balance (PALR Max/Avg). We compare Ring (next-alive) varying virtual nodes per physical node vn (gray dashed) against LRH varying the local candidate count C (blue). We additionally plot MPCH on the same ring size ($vn=256$) while varying probe count $P \in \{2, 4, 8, 16, 32\}$ (red triangles), showing MPCH’s own balance–throughput trade-off under identical failure-handling semantics.

Churn, excess churn, and semantic comparability. Under fixed-candidate liveness failover, LRH achieves 0% excess churn (Theorem 1) and empirically enforces ScanMax= C (8), matching the algorithm’s “exactly C distinct steps” semantics. Rebuild-based methods change candidate sets or lookup tables and therefore may incur excess churn (e.g., Maglev rebuild), consistent with Maglev’s stated disruption trade-offs [8].

6.5 Microbenchmark: MPCH probe generation vs. assignment

A common concern is whether MPCH appears slower due to an unfairly expensive probe-generation implementation. To isolate this, we add a report that measures (i) probe generation only and (ii) assign-only (full mapping) while switching from per-probe mix64 hashing to standard double-hashing. For $N=5000$, $V=256$ ($|\mathcal{R}|=1.28M$), $P=8$, and 2M sampled keys, lower-bound search costs about $\lceil \log_2 |\mathcal{R}| \rceil \approx 21$ steps per probe, i.e., about $P \times 21 \approx 168$ random ring loads per key, or roughly $168 \times 16B \approx 2.62$ KiB of ring-entry traffic per key.

Figure 3 summarizes the microbenchmark breakdown for MPCH.

Table 2: MPCH probe-generation microbenchmark (2M keys; identical across cases). Double-hashing speeds up probe generation by 4.41 \times but improves assign-only throughput by only 1.06 \times , indicating assignment is dominated by $P \times$ lower-bound ring traffic.

Case	Mkeys/s
Assign-only (mix64 probes)	0.81
Assign-only (double-hash probes)	0.86
Probe-gen only (mix64 probes)	75.60
Probe-gen only (double-hash probes)	333.49

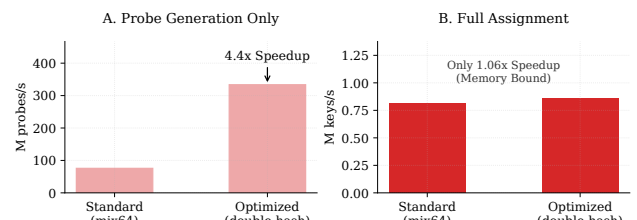


Figure 3: MPCH microbenchmark breakdown: probe generation can be sped up substantially, but assign-only throughput barely changes, indicating lower-bound ring traffic dominates.

This result strengthens the interpretation that MPCH is fundamentally constrained by the microarchitectural cost of repeated lower-bound searches—

scattered ring accesses with data-dependent branches and translation/cache pressure—not by hash arithmetic constants (Section 6.6).

6.6 Microarchitectural attribution with VTune

To connect the access-pattern difference to the throughput gap between MPCH and LRH, we collect Intel VTune hardware-event counters [1, 2] for the same large-scale topology ($N=5000$, $V=256$) and parameters ($P=8$, $C=8$), using $K=5M$ keys to keep profiling overhead manageable. Because the two methods have very different runtimes, we report *normalized rates* (per branch, per cycle, or per retired instruction) rather than raw counts.

Unpredictable control flow from repeated binary searches. MPCH performs P independent lower-bound searches per key; each search is a data-dependent binary search over a large ring array and therefore induces unpredictable branches. Consistent with this structure, Table 3 shows substantially higher branch misprediction rates for MPCH than LRH (2.22× on P-cores; 1.74× on E-cores).

Translation and cache pressure from scattered probes. Binary search touchpoints are scattered across the ring, so repeated searches amplify TLB walks and cache-miss exposure. In our VTune runs, MPCH exhibits higher DTLB walk-active cycles (1.36×) and higher L1D miss-load density (1.63× per retired instruction) on P-cores, with a modest increase in offcore data-read cycles (1.10×). These indicators align with the microbenchmark result in Section 6.5: even large improvements to probe generation do not change the dominant cost in the assignment phase.

Why Top-Down shares can be counterintuitive. In VTune’s Top-Down taxonomy, work executed on wrong-path speculation may still generate cache/TLB pressure, yet the resulting stall time is attributed to *Bad Speculation* rather than *Memory Bound*. Accordingly, Figure 5 shows that MPCH shifts a larger fraction of pipeline slots into Bad Speculation on E-cores, which can make a simple “memory-bound share” argument incomplete for multi-probe binary-search workloads.

Table 3: Selected VTune-derived rates from the same benchmark configuration (normalized to be comparable across different runtimes).

Metric	Core	MPCH	LRH	Ratio
Branch mispredict rate ($\frac{\text{BR_MISP}}{\text{BR_INST}}$)	P	0.161	0.072	2.22
Branch mispredict rate ($\frac{\text{BR_MISP}}{\text{BR_INST}}$)	E	0.158	0.091	1.74
DTLB walk-active cycles / cycles ($\frac{\text{DTLB_WALK_ACTIVE}}{\text{CLK}}$)	P	0.134	0.099	1.36
L1D miss loads / inst retired ($\frac{\text{L1D_MISS_LOAD}}{\text{INST}}$)	P	0.075	0.046	1.63
Offcore data-read cycles / cycles ($\frac{\text{OFFCORE_DATA_RD}}{\text{CLK}}$)	P	0.656	0.598	1.10
TopDown Bad Speculation share (E-core, $\frac{\text{BAD_SPEC}}{\text{sum}}$)	E	0.583	0.350	1.67

Measurement scope. The VTune logs underlying Table 3 and Figure 5 are collected at the process level for the benchmark configuration and include repeated runs; we therefore emphasize normalized rates that are insensitive to wall-time differences. For per-lookup attribution within only the timed query loop, VTune supports scoping counters via ITT task markers; we leave this refinement to future artifact updates.

6.7 Ablation: candidate count C

We vary the number of distinct candidates C under all-alive conditions. Larger C improves balance but reduces throughput, matching the intended trade-off.

6.8 Ablation: ring vnode count V

To quantify how far classical ring hashing can be pushed by increasing vnodes alone, we sweep the number of virtual nodes per physical node V for Ring under the same large-scale setup ($N=5000$, $K=50M$, averaged across failure sizes) and the same failure-handling policy ([next-alive]). Figure 7 shows that increasing V substantially improves balance, but exhibits clear diminishing returns: Max/Avg decreases from 2.6914 ($V=8$) to 1.1118 ($V=1024$), while beyond $V \geq 128$ each doubling improves Max/Avg by only about 4–8% (e.g., 1.3316 → 1.2785 → 1.1826 → 1.1118). At the same time, throughput drops sharply: 131.62 M keys/s ($V=8$) → 67.98 M keys/s ($V=256$) → 36.50 M keys/s ($V=1024$). We report the sweep-run throughput here; the overall suite run in Table 1 reports 68.95 M keys/s at $V=256$ (within 1.4%). This supports a cache/locality interpretation: the ring array grows as $|\mathcal{R}|=N \cdot V$ (a 4× increase from $V=256$ to $V=1024$), making binary searches less cache-friendly and reducing effective memory locality even under `next-alive`.

Build cost also scales with ring size as expected for ring construction: Ring([rebuild]) build time grows from 1.55 ms ($V=8$) to 303.09 ms ($V=1024$, $\approx 195 \times$). Meanwhile, churn remains essentially unchanged across V (about 0.40% in our runs), consistent with the fact that the fraction of keys that must move is primarily determined by the failure fraction rather than token granularity; vnodes mainly influence *how evenly* affected keys are redistributed.

Finally, this sweep strengthens the comparison against simply “turning the vnode knob”: achieving Ring Max/Avg ≈ 1.11 requires $V=1024$ and yields 36.50 M keys/s, whereas LRH at $V=256$ achieves better balance (Max/Avg 1.0947) at higher throughput (60.05 M keys/s, $\approx 1.65 \times$).

Table 4: LRH ablation over C (all-alive). Increasing C improves Max/Avg but decreases throughput.

C	Max/Avg	Thrpt (M/s)
2	1.1871	64.95
4	1.1248	65.09
8	1.0947	60.68
16	1.0679	52.51
32	1.0569	41.20

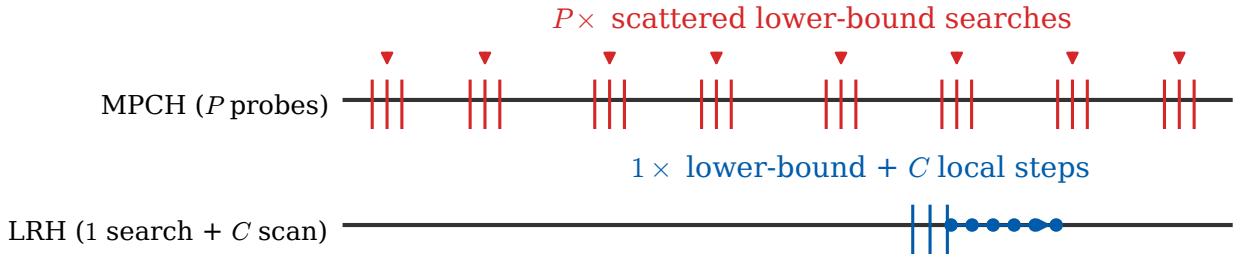


Figure 4: Schematic ring-access traces: MPCH performs P scattered lower-bound searches; LRH performs one lower-bound search plus C local ring steps.

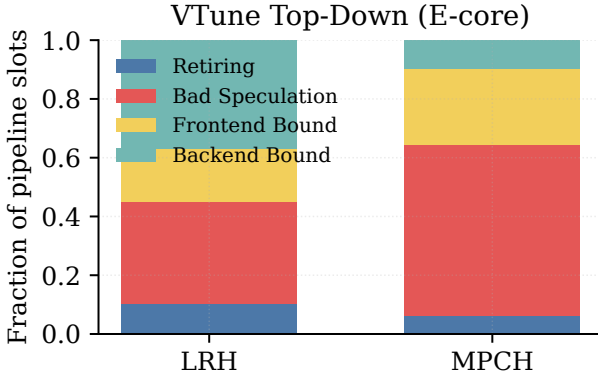


Figure 5: VTune Top-Down breakdown on E-cores (normalized by pipeline slots).

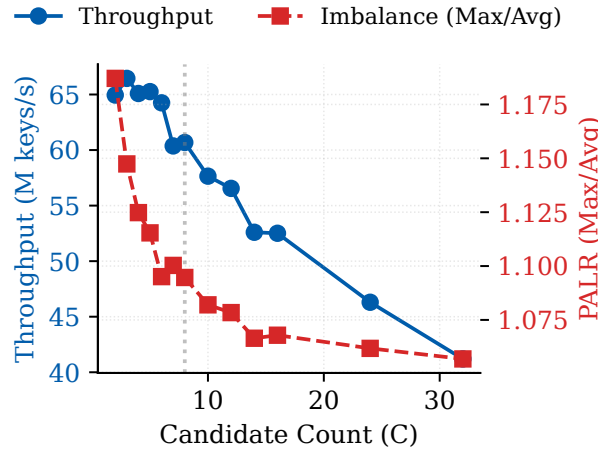


Figure 6: LRH ablation: increasing candidate count C improves balance (Max/Avg) at the cost of throughput.

6.9 Churn by failure size

6.10 Discussion: what the numbers say

Why fixed-candidate works. Fixed-candidate filtering isolates liveness failures from topology changes, enabling Theorem 1. Rebuild changes the candidate sets (or lookup tables), creating additional remapping (excess churn).

Concentration of failover load. LRH reduces concentration compared to ring next-alive: overall $\text{Conc}(\times)$ is 6.14 vs 49.33. This means the busiest receiver of affected keys is closer to an ideal equal split among alive nodes.

Figure 8 shows how concentration evolves with fail-

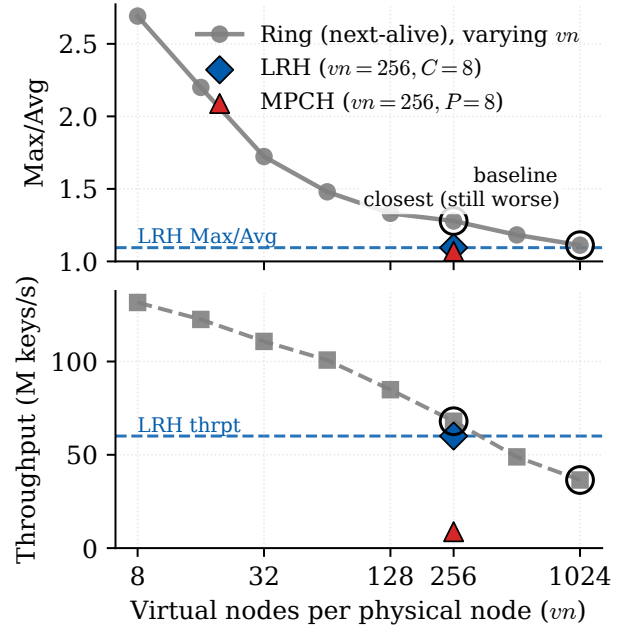


Figure 7: Ring vnode sweep (next-alive): increasing vnodes improves balance with diminishing returns but reduces throughput; overlay points show LRH and MPCDH at $V=256$ for reference.

Table 5: Churn and Excess Churn by Failure Size ($K=50M$).

Algorithm	F=1	F=10	F=50
<i>Churn%</i>			
Ring [next-alive]	0.020	0.201	1.004
LRH [fixed-cand]	0.020	0.200	1.000
<i>Excess%</i>			
Ring [next-alive]	0.000	0.000	0.000
LRH [fixed-cand]	0.000	0.000	0.000
LRH [rebuild]	0.015	0.155	0.765
Maglev [rebuild]	0.145	1.037	3.513
Jump [rebuild-remap]	16.136	83.632	97.657

ure size and highlights LRH’s reduced receiver hot-spotting.

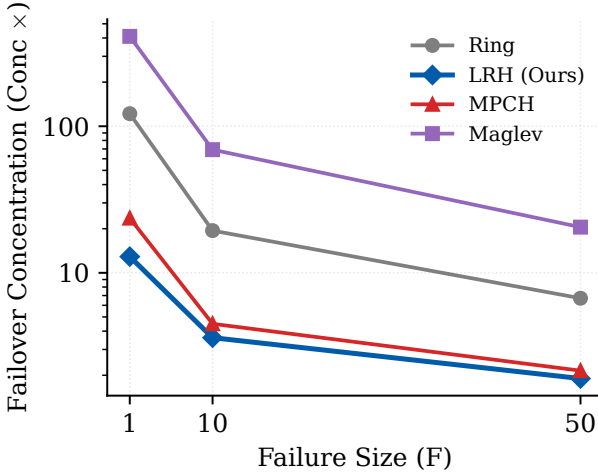


Figure 8: Failover concentration ($\text{Conc} \times$) vs. failure size F (log scale). LRH consistently reduces receiver hot-spotting compared to ring next-alive.

Interpretation of Jump. Under rebuild-by-renumber semantics, Jump shows extreme churn. This reflects a semantic mismatch: Jump is designed for sequential bucket IDs and is not intended for arbitrary deletion/rename membership semantics [12].

6.11 Membership changes: add/remove 1% of nodes

Our strongest guarantee targets liveness changes under fixed topology. For completeness, we also measure membership changes that rebuild data structures. We add/remove 1% of nodes ($N=5000 \rightarrow 5050$ and $N=5000 \rightarrow 4950$).

Figure 9 visualizes churn/excess churn under $\pm 1\%$ membership changes.

These results highlight a semantic distinction: fixed-topology liveness handling can achieve zero excess churn (Theorem 1), whereas membership changes that rebuild candidate sets or tables may introduce excess

Table 6: Membership change (rebuild semantics): churn and excess churn under $\pm 1\%$ node changes.

Algorithm	Churn%	Excess%
<i>+1.00% nodes ($5000 \rightarrow 5050$)</i>		
LRH($vn=256, C=8$)	1.750	0.760
Ring($vn=256$)	0.992	0.000
Maglev($M=65537$)	4.247	3.331
<i>-1.00% nodes ($5000 \rightarrow 4950$)</i>		
LRH($vn=256, C=8$)	1.766	0.765
Ring($vn=256$)	1.004	0.000
Maglev($M=65537$)	4.511	3.513

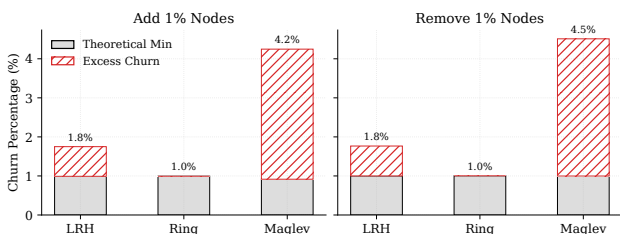


Figure 9: Membership change (rebuild semantics): churn and excess churn under $\pm 1\%$ node changes.

churn depending on the algorithm.

7 Limitations and Future Work

Binary search locality. Although candidate enumeration is strictly C ring steps, the lower-bound search costs $O(\log |\mathcal{R}|)$ accesses. Future work can explore cache-friendly layouts (e.g., Eytzinger layout) [10, 11] or coarse indexing to reduce this cost.

Membership changes. Our strongest churn guarantee is for liveness failures under fixed topology. Membership changes alter the ring and may induce additional churn. We report $\pm 1\%$ membership changes in Section 6.11; broader sweeps (larger percentages and more workloads) remain important for a full comparison with ANCHORHASH [13] and table-based approaches [8]. More broadly, ANCHORHASH is explicitly optimized for *arbitrary membership* updates; our membership experiments use a ring rebuild semantics and should not be read as a like-for-like evaluation of ANCHORHASH’s strengths in that regime.

Weighted accuracy. Weighted HRW is standard [3]. However, in LRH weights interact with the candidate generation mechanism. A dedicated weighted evaluation (e.g., Zipf weights, bimodal capacities) is planned to quantify allocation error vs C .

Implementation optimization. Our implementations prioritize semantic fidelity over peak optimization. Throughput results may vary under optimized production implementations; future work includes more aggressive optimizations and comparisons with highly tuned baselines.

8 Related Work

Consistent hashing and vnodes. Consistent hashing originates with Karger et al. [9]. MPCH provides a widely cited analysis of imbalance and vnode cost [4]. Jump discusses constraints (sequential buckets) and contrasts memory behavior with ring/vnode tables [12].

Rendezvous hashing and weights. HRW (Rendezvous hashing) is described by Thaler and Ravishankar [19]. Weighted variants are standardized in an IETF draft [3].

Bounded loads. CH-BL bounds maximum load under updates using forwarding and provides rigorous expected move bounds with a tunable parameter $c = 1 + \epsilon$ [14].

Modern consistent hashing systems. ANCHORHASH provides a scalable consistent hash with strong consistency under arbitrary membership changes [13]. LRH targets a different trade-off: bounded candidate work and cache-local lookup paths

with explicit liveness failure semantics. In ring-centric deployments, this can translate into a smaller implementation delta: LRH reuses the existing ring layout and changes only the *choice rule* (a C -way local HRW election), whereas adopting ANCHORHASH may require replacing ring-specific data structures and operational conventions.

Table-based balancers. Maglev [8] achieves near-perfect balance via a lookup table and characterizes disruption under backend changes.

Multiple choice intuition. Classical “power of two choices” results explain why comparing a small set of candidates reduces imbalance under suitable sampling assumptions [15]. LRH differs in that candidates are ring-local and engineered for cache locality.

Topology-aware placement. CRUSH [20] is a decentralized hierarchy-aware placement algorithm; our CRUSH-like baseline models a rack hierarchy.

9 Conclusion

LRH reconciles a common systems tension: ring-based schemes are stable but can be imbalanced without large vnode state, while multi-probe/table approaches improve balance at the cost of scattered probes or disruption under rebuild. LRH restricts HRW to a cache-local window of C distinct neighbors and uses next-distinct offsets to bound enumeration to exactly C ring steps. In a large-scale benchmark ($N=5000$, $V=256$, $K=50M$, $C=8$), LRH reduces Max/Avg from 1.2785 to 1.0947 while preserving 0% excess churn under fixed-candidate liveness failover, and empirically enforces ScanMax= C via next-distinct offsets. LRH achieves 60.05 M keys/s, only modestly below Ring(next-alive) at 68.95 M keys/s, and provides $\approx 6.8 \times$ the throughput of MPCH ($P=8$) in our implementation while approaching MPCH’s load balance.

References

- [1] Intel VTune profiler. <https://www.intel.com/content/www/us/en/developer/tools/oneapi/vtune-profiler.html>. Accessed 2025-12-28.
- [2] Get started with intel® vtune™ profiler (2025.0). Intel official PDF guide. https://cdrdv2-public.intel.com/835465/vtune-profiler_get-started-guide_2025.0-769038-835465.pdf, 2025. Accessed 2025-12-28.
- [3] Weighted HRW and its applications. Internet-Draft, IETF. <https://datatracker.ietf.org/doc/html/draft-ietf-bess-weighted-hrw-02>, July 2025. draft-ietf-bess-weighted-hrw-02 (work in progress). Accessed 2025-12-28.
- [4] Ben Appleton and Michael O’Reilly. Multi-probe consistent hashing. arXiv:1505.00062, 2015.
- [5] Jean-Philippe Aumasson and Daniel J. Bernstein. SipHash: A fast short-input PRF. In *Progress in Cryptology – INDOCRYPT 2012*, volume 7668 of *Lecture Notes in Computer Science*, pages 489–508, 2012.
- [6] Giuseppe DeCandia, Deniz Hastorun, Madan Jampani, Gunavardhan Kakulapati, Avinash Lakshman, Alex Pilchin, Swaminathan Sivasubramanian, Peter Vosshall, and Werner Vogels. Dynamo: Amazon’s highly available key-value store. In *Proceedings of the 21st ACM SIGOPS Symposium on Operating Systems Principles (SOSP ’07)*, pages 205–220, 2007.
- [7] Pavlos S. Efraimidis and Paul G. Spirakis. Weighted random sampling with a reservoir. *Information Processing Letters*, 97(5):181–185, 2006.
- [8] Danielle E. Eisenbud, Cheng Yi, Carlo Contavalli, Cody Smith, Roman Kononov, Eric Mann-Hielscher, Ardas Cilingiroglu, Bin Cheyney, Wentao Shang, and Jannah Dylan Hosein. Maglev: A fast and reliable software network load balancer. In *13th USENIX Symposium on Networked Systems Design and Implementation (NSDI 16)*, pages 523–535, 2016.
- [9] David Karger, Eric Lehman, Tom Leighton, Matthew Levine, Daniel Lewin, and Rina Panigrahy. Consistent hashing and random trees: Distributed caching protocols for relieving hot spots on the world wide web. In *Proceedings of the 29th Annual ACM Symposium on Theory of Computing (STOC ’97)*, pages 654–663, 1997.
- [10] Paul-Virak Khuong and Pat Morin. Array layouts for comparison-based searching. arXiv:1509.05053, 2015.
- [11] Paul-Virak Khuong and Pat Morin. Array layouts for comparison-based searching. *ACM Journal of Experimental Algorithms*, 22, 2017.
- [12] John Lamping and Eric Veach. A fast, minimal memory, consistent hash algorithm. arXiv:1406.2294, 2014.
- [13] Gal Mendelson, Shay Vargaftik, Katherine Barabash, Dean H. Lorenz, Isaac Keslassy, and Ariel Orda. AnchorHash: A scalable consistent hash. *IEEE/ACM Transactions on Networking*, 29(2):517–528, 2021.
- [14] Vahab S. Mirrokni, Mikkel Thorup, and Morteza Zadimoghaddam. Consistent hashing with bounded loads. In *Proceedings of the Twenty-Ninth Annual ACM-SIAM Symposium on Discrete Algorithms (SODA 2018)*, pages 587–604, 2018.
- [15] Michael Mitzenmacher. The power of two choices in randomized load balancing. *IEEE Transactions on Parallel and Distributed Systems*, 12(10):1094–1104, 2001.

- [16] Rayon Contributors. Rayon: Data parallelism in rust. <https://docs.rs/crate/rayon/latest>. Accessed 2025-12-28.
- [17] Christian Schindelhauer and Gunnar Schomaker. Weighted distributed hash tables. In *Proceedings of the 17th ACM Symposium on Parallelism in Algorithms and Architectures (SPAA 2005)*, pages 218–227, 2005.
- [18] David G. Thaler and Chinya V. Ravishankar. A name-based mapping scheme for rendezvous. Technical Report CSE-TR-316-96, University of Michigan, 1996. <https://web.eecs.umich.edu/~ravishan/papers/mapping.ps>. Accessed 2025-12-28.
- [19] David G. Thaler and Chinya V. Ravishankar. Using name-based mappings to increase hit rates. *IEEE/ACM Transactions on Networking*, 6(1):1–14, 1998.
- [20] Sage A. Weil, Scott A. Brandt, Ethan L. Miller, and Carlos Maltzahn. CRUSH: Controlled, scalable, decentralized placement of replicated data. In *Proceedings of the 2006 ACM/IEEE Conference on Supercomputing (SC '06)*, 2006.

Appendix A: Reproduction Parameters

```
--nodes 5000 --keys 5000000 --vnodes 256
--candidates 8 --maglev-m 65537
--fail-list 1,10,50 --repeats 5 --warmup 1
--seed 20251226 --threads 0
--hrw-full-max-n 2000 --hrw-sample-keys 200000
--max-scan 4096 --mp-probes 8
--crush-rack-size 50 --crush-bucket-probes 8
--crush-leaf-probes 8 --crush-tries 16
--report-memory --report-mpch-probe-gen --report-membership
--membership-pct 1.0 --ablation-c-list 2,4,8
```

Appendix B: MPCH Sensitivity to Ring Size

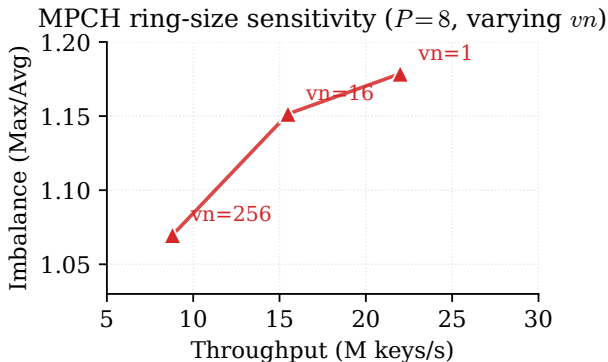


Figure 10: MPCH sensitivity to ring size (vn). We fix $P=8$ and vary $vn \in \{1, 16, 256\}$, isolating ring-size effects from the multi-probe mechanism.

Appendix C: Per-Failure Detailed Tables

Table 7: Detailed Results (failed_nodes=1), averaged over 5 repeats (K=50M).

Algorithm	K	Build	Query	Thrpt	Max/Avg	P99/Avg	CV	Churn%	Excess%	FailAff	MaxRecv	Conc	ScanAvg	ScanMax
Ring(vn=256)[rebuild]	50M	60.57	1304.71	38.33	1.2785	1.1550	0.0639	0.020	0.000	9948	0.0244	121.86	0.00	0
Ring(vn=256)[next-alive]	50M	0.00	717.00	69.74	1.2785	1.1550	0.0639	0.020	0.000	9948	0.0244	121.86	1.00	2
MPCH(ring,vn=256,P=8)[next-alive]	50M	30.20	5660.70	8.84	1.0697	1.0439	0.0192	0.020	0.000	10075	0.0047	23.61	8.00	10
LRH(vn=256,C=8)[fixed-cand]	50M	30.01	819.54	61.02	1.0947	1.0574	0.0244	0.20	0.000	9927	0.0026	12.90	8.00	8
LRH(vn=256,C=8)[rebuild]	50M	64.53	1511.57	33.12	1.0947	1.0574	0.0244	0.035	0.015	9927	0.0025	12.40	8.00	8
Jump[rebuild-buckets]	50M	0.00	210.29	238.02	1.0361	1.0232	0.0100	16.156	16.136	10035	1.0000	4999.00	0.00	0
Maglev(M=65537)[rebuild]	50M	3.12	37.39	1339.74	1.1000	1.0818	0.0257	0.165	0.145	9825	0.0821	410.42	0.00	0
HRW(sample K=2M)	2M	0.01	1742.41	1.15	1.1810	1.1185	0.0501	0.020	0.000	395	0.0056	28.02	0.00	0
CRUSH-like(rack=50,bp=8,lp=8,tries=16)	50M	0.00	601.80	83.17	1.0379	1.0233	0.0100	0.020	0.000	9994	0.0009	4.40	16.00	45

Table 8: Detailed Results (failed_nodes=10), averaged over 5 repeats (K=50M).

Algorithm	K	Build	Query	Thrpt	Max/Avg	P99/Avg	CV	Churn%	Excess%	FailAff	MaxRecv	Conc	ScanAvg	ScanMax
Ring(vn=256)[rebuild]	50M	60.03	1310.51	38.18	1.2785	1.1550	0.0639	0.201	0.000	100424	0.0039	19.41	0.00	0
Ring(vn=256)[next-alive]	50M	0.00	723.17	69.14	1.2785	1.1550	0.0639	0.201	0.000	100424	0.0039	19.41	1.00	3
MPCH(ring,vn=256,P=8)[next-alive]	50M	28.34	5713.26	8.75	1.0697	1.0439	0.0192	0.201	0.000	100316	0.0009	4.49	8.01	11
LRH(vn=256,C=8)[fixed-cand]	50M	31.66	833.66	59.98	1.0947	1.0574	0.0244	0.200	0.000	100123	0.0007	3.61	8.00	8
LRH(vn=256,C=8)[rebuild]	50M	58.39	1509.31	33.16	1.0947	1.0574	0.0244	0.355	0.155	100123	0.0007	3.36	8.00	8
Jump[rebuild-buckets]	50M	0.00	205.89	244.34	1.0361	1.0232	0.0100	83.831	83.632	99780	0.1015	506.39	0.00	0
Maglev(M=65537)[rebuild]	50M	2.88	38.37	1304.23	1.1000	1.0818	0.0257	1.237	1.037	99890	0.0139	69.23	0.00	0
HRW(sample K=2M)	2M	0.01	1715.48	1.17	1.1810	1.1185	0.0501	0.199	0.000	3989	0.0015	7.51	0.00	0
CRUSH-like(rack=50,bp=8,lp=8,tries=16)	50M	0.00	605.60	82.61	1.0379	1.0233	0.0100	0.200	0.000	99884	0.0004	1.92	16.02	58

Table 9: Detailed Results (failed_nodes=50), averaged over 5 repeats (K=50M).

Algorithm	K	Build	Query	Thrpt	Max/Avg	P99/Avg	CV	Churn%	Excess%	FailAff	MaxRecv	Conc	ScanAvg	ScanMax
Ring(vn=256)[rebuild]	50M	62.34	1296.59	38.57	1.2785	1.1550	0.0639	1.004	0.000	501760	0.0014	6.71	0.00	0
Ring(vn=256)[next-alive]	50M	0.00	735.85	67.95	1.2785	1.1550	0.0639	1.004	0.000	501760	0.0014	6.71	1.01	4
MPCH(ring,vn=256,P=8)[next-alive]	50M	27.55	5668.07	8.82	1.0697	1.0439	0.0192	1.001	0.000	500370	0.0004	2.15	8.04	13
LRH(vn=256,C=8)[fixed-cand]	50M	30.06	845.75	59.16	1.0947	1.0574	0.0244	1.000	0.000	500198	0.0004	1.90	8.00	8
LRH(vn=256,C=8)[rebuild]	50M	65.11	1508.54	33.20	1.0947	1.0574	0.0244	1.766	0.765	500198	0.0004	1.93	8.00	8
Jump[rebuild-buckets]	50M	0.00	191.22	261.92	1.0361	1.0232	0.0100	98.656	97.657	499604	0.0205	101.30	0.00	0
Maglev(M=65537)[rebuild]	50M	2.93	39.79	1261.32	1.1000	1.0818	0.0257	4.511	3.513	498759	0.0041	20.50	0.00	0
HRW(sample K=2M)	2M	0.01	1712.20	1.17	1.1810	1.1185	0.0501	0.997	0.000	19935	0.0007	3.28	0.00	0
CRUSH-like(rack=50,bp=8,lp=8,tries=16)	50M	0.00	605.71	82.60	1.0379	1.0233	0.0100	0.999	0.000	499552	0.0003	1.41	16.08	67

Appendix D: Critical Modeling Boundaries and More Rigorous Derivations

This appendix refines the main-text scaling arguments by making explicit: (i) randomness of the candidate-coverage count d_n (compound variance), (ii) discrete key sampling noise vs. structural imbalance, (iii) locality-induced correlations, and (iv) the impact of rack-correlated failures. The goal is to *bound* the terms omitted by simplified derivations and clarify when they are negligible.

D.1 Setup and the structural smoothing identity

Let $m = NV$ be the number of ring tokens and let G_1, \dots, G_m be the cyclic gaps. For each gap i , let S_i be the C distinct LRH candidates. Let L_n denote node n 's fluid load share.

Lemma 2 (Uniform HRW winner within a set). *Fix a key k and a candidate set S with $|S| = C$. If $\{s(k, n)\}_{n \in S}$ are i.i.d. continuous random variables, then each $n \in S$ wins with probability $1/C$.*

Lemma 3 (Local averaging (load linearization)). *Under Lemma 2, the fluid load satisfies*

$$L_n = \frac{1}{C} \sum_{i: n \in S_i} G_i.$$

D.2 Dirichlet gaps and the missing “compound variance” term

Assume token positions are i.i.d. uniform on $[0, 1]$ and then sorted. Then

$$(G_1, \dots, G_m) \sim \text{Dirichlet}(1, \dots, 1). \quad (2)$$

Let $I_n := \{i : n \in S_i\}$ and $d_n := |I_n|$. A subtlety is that d_n is generally *random* (depending on local token layout and the “distinct” constraint), so L_n is a mixture over d_n . We now make the variance decomposition explicit.

Proposition 1 (Conditional Beta and total variance decomposition). *Under (2), conditional on I_n (equivalently on d_n),*

$$\begin{aligned} \sum_{i \in I_n} G_i \mid I_n &\sim \text{Beta}(d_n, m - d_n), \\ L_n \mid d_n &\sim \frac{1}{C} \text{Beta}(d_n, m - d_n). \end{aligned}$$

Moreover,

$$\text{Var}(L_n) = \mathbb{E}[\text{Var}(L_n \mid d_n)] + \text{Var}(\mathbb{E}[L_n \mid d_n]). \quad (3)$$

Why the second term exists. Because $\mathbb{E}[\text{Beta}(d, m - d)] = d/m$, we have

$$\mathbb{E}[L_n \mid d_n] = \frac{d_n}{Cm}.$$

Therefore the “missing” compound term is

$$\text{Var}(\mathbb{E}[L_n \mid d_n]) = \frac{\text{Var}(d_n)}{C^2 m^2}. \quad (4)$$

D.3 Bounding $\text{Var}(d_n)$ when $C \ll N$

The distinct-candidate rule implies d_n can drop below VC if multiple tokens of the same node fall within the same “ C -distinct” neighborhood, causing overlapping coverage intervals. We do not attempt an exact law for d_n ; instead we give a conservative bound.

A simple collision proxy. For each token occurrence of node n , consider the event that node n appears again before the scan collects C *distinct* nodes ahead. Let $Y_t \in \{0, 1\}$ be the indicator for the t -th token of node n that such a “self-collision” occurs. Define $Y := \sum_{t=1}^V Y_t$. A self-collision implies that the coverage contribution of the colliding token partially overlaps with its predecessor. Conservatively, each such event reduces the ideal coverage count VC by at most C . Thus,

$$0 \leq VC - d_n \leq CY. \quad (5)$$

Lemma 4 (Self-collision probability scale). *Under uniform random token placement and $C \ll N$, one has*

$$\mathbb{E}[Y_t] \lesssim \frac{C}{N}, \quad \text{hence} \quad \mathbb{E}[Y] \lesssim \frac{VC}{N}.$$

Variance bound (rare-collision regime). Lemma 4 gives $\mathbb{E}[Y] \lesssim VC/N$. Moreover, in the same randomized-ring regime collisions are rare and local; consequently Y behaves like a Poisson-binomial count and concentrates at its mean. A conservative second-moment bound yields

$$\text{Var}(Y) = O(\mathbb{E}[Y]) = O\left(\frac{VC}{N}\right).$$

This holds, for example, when $VC/N = O(1)$. Plugging into (5) gives:

$$\text{Var}(d_n) \leq C^2 \text{Var}(Y) \lesssim \frac{VC^3}{N}. \quad (6)$$

Impact on $\text{Var}(L_n)$. Plugging (6) into (4) with $m = NV$ yields

$$\text{Var}(\mathbb{E}[L_n \mid d_n]) = \frac{\text{Var}(d_n)}{C^2 m^2} \lesssim \frac{VC^3/N}{C^2 (N^2 V^2)} = \frac{C}{N^3 V}.$$

Compared to the leading structural term $\mathbb{E}[\text{Var}(L_n \mid d_n)] \approx \mathbb{E}[d_n]/(C^2 m^2) \approx 1/(N^2 VC)$, the ratio is on the order of C^2/N . Equivalently, since both terms share the denominator $C^2 m^2$, the compound/structural ratio is $\text{Var}(d_n)/\mathbb{E}[d_n] = O(C^2/N)$ under (6). Thus, for large clusters ($C^2 \ll N$), the randomness of d_n is a negligible second-order effect.

D.4 Fluid load vs. discrete keys

The main text analyzes *structural* imbalance (L_n). Real systems have K discrete keys, introducing sampling noise (X_n).

$$\begin{aligned} \text{Var}(X_n) &= K \mathbb{E}[L_n(1 - L_n)] \quad (\text{sampling}) \\ &\quad + K^2 \text{Var}(L_n) \quad (\text{structural}). \end{aligned} \quad (7)$$

For large K per node ($K/N \gg 1$), the structural term dominates, justifying our focus on smoothing L_n .

D.5 Locality correlations

Neighboring nodes have overlapping candidate windows, making (L_n) positively correlated. This does *not* invalidate union bounds used for PALR (Theorem 5), as $\Pr[\cup A_n] \leq \sum \Pr[A_n]$ holds regardless of independence. Correlation implies that if overload occurs, it may manifest as a local cluster of loaded nodes rather than isolated spikes.

D.6 Baseline fairness: statistical equivalence vs. cost

We emphasize that while LRH is statistically equivalent to increasing vnodes to $V' = VC$, it achieves this without the $C \times$ memory and build-time penalty associated with expanding the ring structure. It decouples the smoothing parameter (C) from the ring state size (NV).

D.7 Rack-correlated failures

Theorem 2 assumes independent failures. In practice, failures may be correlated by topology (e.g., a top-of-rack switch failure). Let the cluster consist of N nodes partitioned into racks of size R . Suppose a full rack fails (batch failure of R nodes).

Because tokens are placed via a hash function that is agnostic to rack ID (Random Hashing), the relative positions of tokens from a specific rack are random uniform. Consequently, the set of candidates S_k for any key k (which consists of C logically consecutive distinct nodes) is effectively a random sample of size C from the population of N nodes, with respect to rack affiliation.

We can thus apply Theorem 3 (Fixed- F model) with $F = R$:

$$\Pr[\text{all } C \text{ candidates are in the failed rack}] \approx \left(\frac{R}{N}\right)^C.$$

For typical values (e.g., $R = 40, N = 5000, C = 8$), this probability is $(0.008)^8 \approx 10^{-17}$, which is negligible. This result confirms that LRH maintains high availability under rack failures without requiring explicit cross-rack placement constraints, provided standard random hashing is used.